

IMPROVEMENTS IN LONGITUDINAL PHASE SPACE TOMOGRAPHY AT PITZ

N. Aftab*, Z. Aboulbanine, P. Boonpornprasert, G. Georgiev, J. Good, M. Gross, A. Hoffmann, M. Krasilnikov, X.-K. Li, A. Lueangaramwong, R. Niemczyk, A. Oppelt, H. Qian, C. Richard, F. Stephan, G. Vashchenko, Deutsches Elektronen-Synchrotron DESY, Zeuthen, Germany
W. Hillert, University of Hamburg, Institute for Experimental Physics, Hamburg, Germany
A. J. Reader, School of Biomedical Engineering and Imaging Sciences, King's College London, UK

Abstract

Methodical studies to improve the longitudinal phase space (LPS) tomography of space-charge dominated electron beams were carried out at the Photo Injector Test facility at DESY in Zeuthen (PITZ). An analytical model was developed to quantify mean momentum, RMS energy spread, bunch length and phase advance. Phase advance analysis determined the booster phase scan range and step size to be used for obtaining momentum projections. A slit was introduced before the booster to truncate the beam in transverse plane to strongly reduce the space charge effects. The signal resolution of this truncated beam was improved by careful beta function control at the reference screen of the momentum measurements. The reconstruction algorithm was changed from Algebraic Reconstruction Technique (ART) to Image Space Reconstruction Algorithm (ISRA) owing to its assurance of non-negative solutions. In addition, the initial physically justified assumption of LPS, based on low-energy section measurements, was established to clear out noise-like artefacts. This paper will highlight the improvements made in the LPS tomography and compare the simulated and experimental results.

INTRODUCTION

Free-electron Lasers (FELs) require high-brightness electron beams to generate coherent radiation with short wavelength and high intensity. The Photo Injector Test facility at DESY in Zeuthen (PITZ) was established as a test stand of high-brightness electron sources for the European XFEL and FLASH [1]. The PITZ beamline consists of a normal conducting L-band 1.6-cell copper gun cavity with a Cs_2Te photocathode that produces ~ 6.5 MeV electron bunches with variable bunch lengths and up to several nC charge. The electron beam is further accelerated by a cut-disc type accelerating structure called booster, to an energy of up to ~ 20 MeV. Downstream the booster, the beamline consists of different diagnostics for detailed measurements of the electron beam properties. The transverse phase space characterization of the beam is done using a slit scan technique [2]. The longitudinal phase space (LPS) characterization is done using a transverse deflecting structure [3]. To determine LPS of the beam before the booster, a tomographic reconstruction technique is applied [4]. Figure 1 shows the PITZ beamline till the high energy spectrometer.

* namra.aftab@desy.de

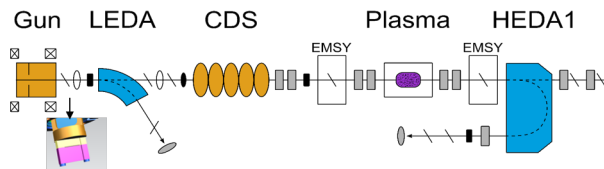


Figure 1: PITZ beamline till the high energy spectrometer with a slit shown at the first screen station after the gun.

The results of tomography obtained by the existing method has many artefacts and hence overestimates the longitudinal emittance. A hard charge cut is applied on the reconstructed LPS to give correct values. Also, the reconstruction results are more accurate for low-charge beams ~ 10 pC since space-charge forces are not catered for the algorithm. Typically, 250 pC beams are characterized at PITZ since this is the working point of the European XFEL.

In this paper, the procedure adopted in the experiment for obtaining the momentum projections for 250 pC beam will be explained. The optimized projections are fed to an Image Space Reconstruction Algorithm (ISRA) [5]. The algorithm will be described as well as the formulation of the initial estimate for the iterations. This initial estimate is built from the low energy section and plays a vital role for reliable reconstruction. An analytical model to understand the longitudinal phase advance of the beam is also described. The paper discusses the improvements made in the LPS tomography and compares the simulated and experimental results.

LPS MODELLING

The particle motion can be characterized in LPS by the momentum p_z of the particle corresponding to the phase of the booster. This can be used to understand and quantify the quality of an electron beam for accelerator design and phase space manipulations. To derive an analytical model for such a beam, the distribution of the particles can be approximated by an ellipse with some correlation as shown in Fig. 2.

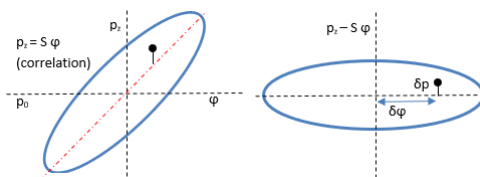


Figure 2: LPS with correlation (left) w/o correlation (right).

If we consider a particle with an initial momentum from the electron gun p_z^{gun} is being accelerated by the booster, then the final momentum of the particle p_z^{boo} can be calculated by Eq. (1):

$$p_z^{\text{boo}} = p_z^{\text{gun}} + S\delta\varphi + \delta p + V\cos(\varphi + \delta\varphi), \quad (1)$$

where, S is the LPS linear chirp that defines the correlation, V is the momentum gain by the booster, φ is the phase of the booster w.r.t. maximum mean momentum gain phase and the (x, y) co-ordinates of the particle in the phase space ellipse are shown by $(\delta\varphi, \delta p)$. The average beam momentum after the booster can be found by integrating all the particles in the phase space ellipse. After a few mathematical steps, we derive Eq. (2):

$$\langle p_z^{\text{boo}} \rangle = p_z^{\text{gun}} + V\cos\varphi(1 - \sigma_\varphi^2/2). \quad (2)$$

The RMS momentum spread can be found by subtracting the mean momentum from the momentum distribution. It is expressed in Eq. (3) as:

$$\sigma_p^2 = \sigma_{p_{\min}}^2 + V^2(\sin\varphi - \sin(\varphi - \sigma_\varphi))\sigma_{p_{\min}})^2\sigma_\varphi^2. \quad (3)$$

From Eq. (2) and (3), we can derive Eq. (4) that gives bunch length:

$$\sigma_\varphi = \sigma_p/|V\sin\varphi|. \quad (4)$$

The phase advance Φ of the phase space ellipse can be calculated by using the bunch length and the minimum RMS energy spread. The formula is shown in Eq. (5):

$$\Phi = \tan^{-1}(S\sigma_\varphi/\sigma_{p_{\min}}), \quad (5)$$

where S is the slope of the LPS. In experiment, we can use the modelled energy spread as slope and find the beam phase advance. As the booster phase varies, the beam phase advance is significant around the minimum energy spread and decreases gradually as the energy spread increases. This trend can be seen by plotting RMS energy spread relative to its minimum against phase advance. Note that this model does not take space charge effects into account.

EXPERIMENT OPTIMIZATION

The experiment was conducted for a 250 pC beam produced by ~6.6 ps FWHM laser and accelerated up to 16.95 MeV. The measurement procedure consists of the following steps:

- Low energy dispersive arm (LEDA) section was used to scan the gun phase and find the corresponding mean momentum and momentum spread as shown in Fig. 3.
- Since the beam is space-charge dominated, it was chopped transversely by inserting a 200 μm -wide slit after the gun to strongly reduce the space charge effects. Figure 1 shows the location of the slit.
- A solenoid scan was done to obtain approximately 10 pC after the slit.
- A steerer was used to vertically center the beam on the reference screen for the momentum measurements.

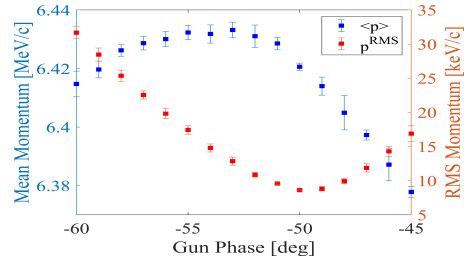


Figure 3: Low energy momentum scan.

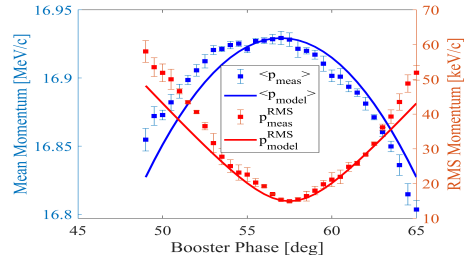


Figure 4: High energy momentum scan and the fitted model.

- High energy dispersive arm (HEDA1) was used to do a rough scan of the booster phase to find the optimum phase range and step size for reconstruction.
- The booster phase scan was repeated and the corresponding momentum projections were saved after focusing the beam on the reference screen for improved resolution.

Figure 4 shows the mean momentum and momentum spread corresponding to each booster phase.

The model fits well to the measured data around the maximum mean momentum and the minimum energy spread but there is some discrepancy at the off-centre phases. This is due to the deviation of the beam trajectories in the dipole for the off-crest phases causing systematic error in the measurement. This error can be removed by centring the beam on the momentum measurement screen by adjusting the dipole current for every booster phase.

Figure 5 shows the relative momentum spread corresponding to the phase advance. The phase advance varies significantly around 70° until 1.5 keV and then until 3 keV the change is gradual $\sim 10^\circ$. After 3 keV the phase advance is almost negligible. The momentum projections for tomography should correspond to the booster phase range which covers the whole LPS phase advance and the step size should be optimized in order to produce a smooth curve.

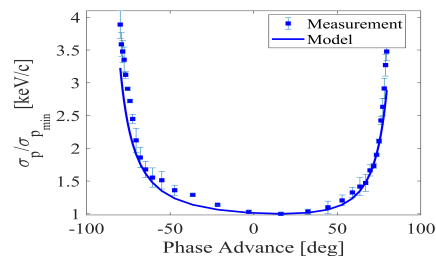


Figure 5: Phase advance from measurement and fitted model.

RECONSTRUCTION ALGORITHM

A variety of techniques have been developed to reconstruct higher dimensional distributions from lower dimensional projections, commonly known as tomography [6]. Tomography often involves an image (or object representation) reconstruction technique that utilizes projections of the object from different viewing angles and then uses iterative equation solving methods e.g. maximum entropy technique (MENT) [7] or algebraic reconstruction technique (ART) [8] to reconstruct the original distribution.

Image Space Reconstruction Algorithm (ISRA)

ISRA is a non-negative multiplicative least squares algorithm and is derivable from a least squares objective function [9]. The equation for ISRA is expressed as:

$$x^{k+1} = x^k \frac{A^T m}{A^T A x^k}, \quad (6)$$

where x^k is a vector containing the current estimate of reconstructed phase space and x^{k+1} is the next update, m is a vector that contains projections corresponding to all booster phases also known as sinogram as shown in Fig. 6, and A is a weight matrix built from the LPS model. The weights are distributed in the neighboring pixels by bilinear interpolation to model the signal analogue to discretization conversion effects.

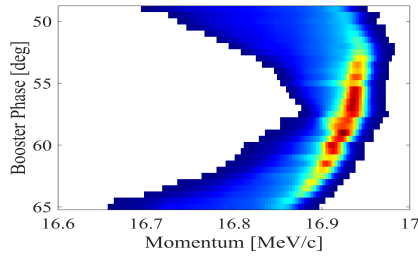


Figure 6: Sinogram.

ISRA takes a current estimate and forward projects it to form a vector Ax^k . This vector is back projected to form a predicted back projected vector. Similarly, the measured projections are also back projected using the system matrix. The ratio of these back projections provides a correction factor to update the current estimate. The initial estimate x^1 vector can be taken as a vector of uniform values (e.g. 1). The iterations are carried out until the root mean square error (RMSE) between measured sinogram and predicted sinogram falls below the tolerance level i.e. 0.5%.

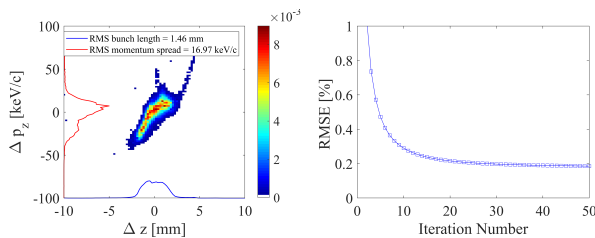


Figure 7: LPS after 50 iterations when $x^1 = 1$ (left) RMSE (right).

Figure 7 shows the reconstructed LPS after 50 iterations. The colorscale shows it is normalized to 1. After ~ 30 iterations, RMSE is already well below the tolerance level ($\sim 0.2\%$) and there are only a few noise artefacts. This can be further improved by using an initial estimate from low energy momentum measurement.

Initial Estimate from LEDA

An initial educated guess of LPS from LEDA was established to further improve the reconstruction results. Basically, the momentum profile at an off-crest phase $\rho_n(p_z)$ was used to select the range of phase from LEDA scan to be used as an initial matrix. Once we had the range, a Gaussian was fit on each of the mean momentum points as shown in Fig. 8. The amplitude of the Gaussians was taken from the weights of off-crest phase momentum profile normalized to 1. The expression for initial guess for LPS can be written mathematically by Eq. (7).

$$LPS(z, p_z) = \sum_{n=1}^N G_n(p_z) \Delta_n(z), \quad (7)$$

where $G_n(p_z)$ is the p_z -distribution for the n^{th} longitudinal slice within the bunch scanned by the step function $\Delta_n(z)$. Equations 8 and 9 show their formulas:

$$G_n(p_z) = \rho_n / (\sqrt{2\pi} \sigma_{pn}) \exp[-(p_z - p_{zn})^2 / (2\sigma_{pn}^2)] \quad (8)$$

$$\Delta_n(z) = 1 / \Delta z, |z - z_n| \leq \Delta z / 2. \quad (9)$$

The reconstructed LPS after 50 iterations starting from a well-defined initial estimate is shown in Fig. 9. The artefacts are almost removed and the overall structure is similar to the uniform initial estimate case. The initial estimate from LEDA not only removes the noise but also impacts the overall distribution of particles in phase space. One can compare the RMS bunch length and energy spread values of reconstructed LPS to note this effect.

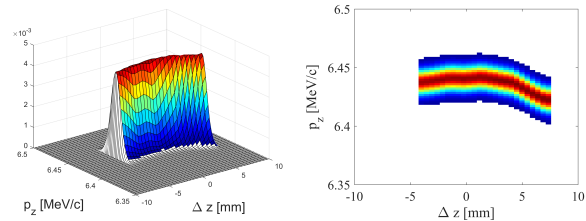


Figure 8: weighted Gaussian p_z -distributions along the bunch at selected LEDA phase range (left) shown as initial estimate (right).

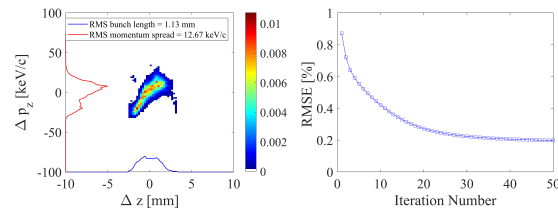


Figure 9: LPS after 50 iterations (left) RMSE (right).

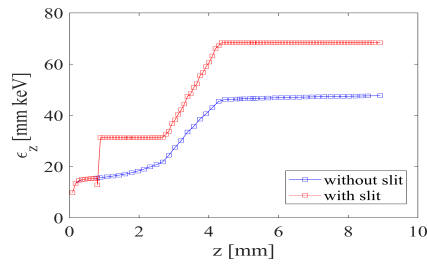


Figure 10: ϵ_z without and with the slit along the beamline. Booster starts at 2.675 m and ends at 4.385 m.

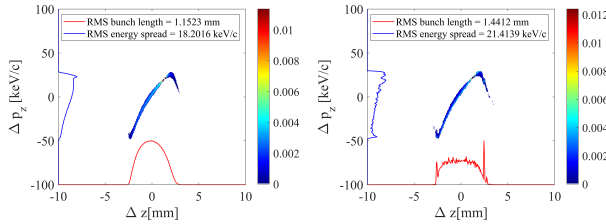


Figure 11: LPS before slit at 0.8 m (left) and after slit at 1.7 m (right).

Comparison with Simulated LPS

A Space Charge Tracking Algorithm (ASTRA) [10] was used to simulate the beam with similar parameters with and without the slit at 0.8 m. It was observed that after inserting the slit, the beam energy and bunch length increased slightly causing increase in the longitudinal emittance along the beamline. Figure 10 shows the plot of the ϵ_z starting from the gun to the high energy section. Figure 11 shows the beam and its projections before the slit at 0.8 m and after the slit at 1.7 m. The weights along the momentum profiles are changed by the introduction of the slit which was used to remove transverse space charge effects. As a result, there is a systematic error introduced because of correlation in p_z and radial plane [11].

Figures 7 and 9 show the reconstructed LPS with bunch length and momentum profiles and corresponding RMS values. The ϵ_z after 50 iterations for uniform initial matrix case is 24.85 mm · keV and for the case with the pre-defined initial matrix from low energy sections is 14.29 mm · keV. The increase in bunch length and energy spread caused by the insertion of the slit is compensated by using the initial estimate from LEDA.

CONCLUSION AND OUTLOOK

Methodical studies for LPS reconstruction via tomography were done that included better signal resolution with careful beta function control with the help of a slit and phase advance analysis during booster phase scan. Another important step

accomplished was artefact-free and improved reconstruction results by using ISRA and an initial estimate from LEDA. A combination of improved experimental conditions and optimized reconstruction algorithm yielded reliable LPS tomography results. The next step would be minimizing the systematic error by centering the beam on the momentum measurement screen for all booster phases as well as using better noise compensation for improved SNR. This would not only decrease the RMSE but also the required number of iterations for convergence.

REFERENCES

- [1] E. J. Jaeschke *et al.*, *Synchrotron Light Sources and Free-Electron Lasers*, Springer Cham, 2016, p. 155. doi: 10.1007/978-3-319-14394-1
- [2] M. Krasilnikov *et al.*, “Experimentally minimized beam emittance from an L-band photoinjector”, *Phys. Rev. ST Accel. Beams*, vol. 15, p. 100701, 2012. doi: 10.1103/PhysRevSTAB.15.100701
- [3] L. V. Kravchuk *et al.*, “Layout of the PITZ Transverse Deflecting System for Longitudinal Phase Space and Slice Emittance Measurements”, in *Proc. LINAC’10*, Tsukuba, Japan, Sep. 2010, paper TUP011, pp. 416–418.
- [4] D. Malyutin, “Time resolved transverse and longitudinal phase space measurements at the high brightness photo injector PITZ”, Ph.D. dissertation, Universität Hamburg, Germany, 2014.
- [5] M. E. Daube-Witherspoon and G. Muehlehner, “An Iterative Image Space Reconstruction Algorithm Suitable for Volume ECT”, *IEEE Trans. Med. Imaging*, vol. 5, pp. 61–66, 1986. doi: 10.1109/TMI.1986.4307748
- [6] A. C. Kak, M. Slaney, *Principles of Computerized Tomographic Imaging*, IEEE Press, 1979.
- [7] S. F. Gull and T. J. Newton, “Maximum entropy tomography”, *Appl. Opt.*, vol. 25, pp. 156–160, 1986. doi: 10.1364/AO.25.000156
- [8] H. Loos *et al.*, “Longitudinal phase space tomography at the SLAC Gun Test Facility and the BNL DUV FEL”, *Nucl. Instrum. Methods Phys. Res., Sect. A*, vol. 528, p. 189, 2004. doi: 10.1016/j.nima.2004.04.044
- [9] A. R. De Pierro, “On the Convergence of the Iterative Image Space Reconstruction Algorithm for Volume ECT”, *IEEE Trans. Med. Imaging*, vol. 6, pp. 174–175, 1987. doi: 10.1109/TMI.1987.4307819
- [10] K. Floettmann, A space charge tracking code - ASTRA, <http://desy.de/~mpyf10>
- [11] H. Qian, *et al.*, “Slice energy spread measurement in the low energy photoinjector”, *Phys. Rev. Accel. Beams*, vol. 25, 2022. doi: 10.1103/PhysRevAccelBeams.25.083401